



CYCLIC LOAD TESTING OF PRECAST HYBRID FRAME CONNECTIONS

Jubum Kim¹, John Stanton², Gregory MacRae³, Stephen Day⁴ and Masahiro Sugata⁵

SUMMARY

The paper describes a new concrete framing system, in which a combination of unbonded post-tensioning and bonded deformed bars is used to provide the flexural resistance between beams and columns. First the characteristics of the system are described. Then tests on four beam-column sub-assemblages are reported. The tests were conducted as proof-of-concept needed to gain regulatory acceptance of the system for use in a 40-story building in San Francisco. The tests were needed because the system does not satisfy all the prescriptive requirements of Chapter 21 of ACI 318-02. The tests showed that the system is capable of providing excellent seismic performance. They also demonstrated some of the critical features that must be attended to properly in design.

INTRODUCTION

Code Requirements for Concrete Frames

The seismic design of reinforced concrete frames in the US is governed by codes such as UBC (“Uniform” 1997) and IBC (“2003 International” 2003). In both cases, the capacity aspect of the design is derived, either directly or by reference, from ACI 318 (“Building” 2002). That document requires that the frame use reinforcement with a yield nominal strength no higher than 60 ksi. This limitation on the yield strength has been in place since 1971, and was introduced to reduce the probability of bar buckling and to ensure dissipation of energy through yielding.

While frames designed according to this philosophy have, in general, performed well over the years, the prescriptive rules in Chapter 21 of ACI 318 have inhibited the development of

¹ Assistant Professor, Dept. of Civil and Env. Eng., Clarkson Univ., Potsdam, NY 13699, USA.

² Professor, Dept. of Civil and Env. Eng., U. of Washington, Seattle, WA 98195-2700, USA.

³ Associate Professor, Dept. of Civil and Env. Eng., U. of Washington, Seattle, WA 98195-2700, USA.

⁴ Structural Engineer, Coughlin Porter Lundeen, Seattle, WA 98101, USA.

⁵ Senior Development Engineer, Takenaka Corp, Tokyo, Japan.

alternative approaches. Section 21.2.1.5 of ACI 318 theoretically offers an opportunity for using a different design philosophy, in that it states:

“A reinforced concrete structural system not satisfying the requirements of this chapter shall be permitted if it is demonstrated by experimental evidence and analysis that the proposed system will have strength and toughness equal to or exceeding those provided by a comparable monolithic reinforced concrete structure satisfying this chapter”.

However, in practice, this procedure has seldom been followed because the strength and toughness of a conforming frame are not defined, and because specific test protocols to demonstrate equivalence did not exist. Any Building Official approving such a system therefore exposed him or herself to significant liability. Furthermore the time required to negotiate an acceptable testing protocol was likely have an adverse, and possibly terminal, effect on the project schedule.

In 2001, ACI published ACI-ITG1.1 (“ACI Innovation” 2001). That document spells out the testing requirements and acceptance criteria for approval of framing systems that do not conform to Chapter 21 of ACI 318, and therefore paves the way for development of new systems. One such system is the Hybrid Frame (Stone et al. 1995). Its development was, in fact, the catalyst for writing ITG1.1. This paper describes the Hybrid Frame system and the testing program that it underwent in accordance with ACI-ITG1.1 in order to allow its use in a 40 story building in San Francisco.

Hybrid Frames

A Precast Hybrid Frame is illustrated in Figure 1. It is a moment frame that is made from precast beams and columns, in which the components are connected by a combination of unbonded post-tensioned tendons and bonded deformed bar steel. Several configurations are possible (Stanton and Nakaki 2002) but, in the one that has been used most often, the columns are continuous over several stories and each beam spans a single bay. The connections are made at the beam-column interface where a grout pad provides the length tolerance needed for erection. This configuration minimizes the number of costly column-to-column connections and leads to the use of line elements, which are relatively simple and economical to transport.

The genesis of the concept lies in tests conducted at the University of Washington (Ishizuka et al. 1984), and its was then developed a period of years with further testing at NIST, sponsored partly by Charles Pankow Builders Ltd (Cheok and Stone 1994), and within the PRESSS Program, sponsored by NSF and PCI (Priestley and MacRae 1996, Nakaki et al. 1999). The concept has also been adapted for use in steel frames (Ricles et al. 2001, Christopoulos et al. 2002).

The principle on which it works is simple, and is shown in Figure 2. The precast components are connected by unbonded prestressing tendons that extend over the length of the frame. The tendon is usually placed at mid-height of the beam, and passes through ducts in the columns and beams. When lateral forces act, the frame deforms by opening of the cracks at the beam-column

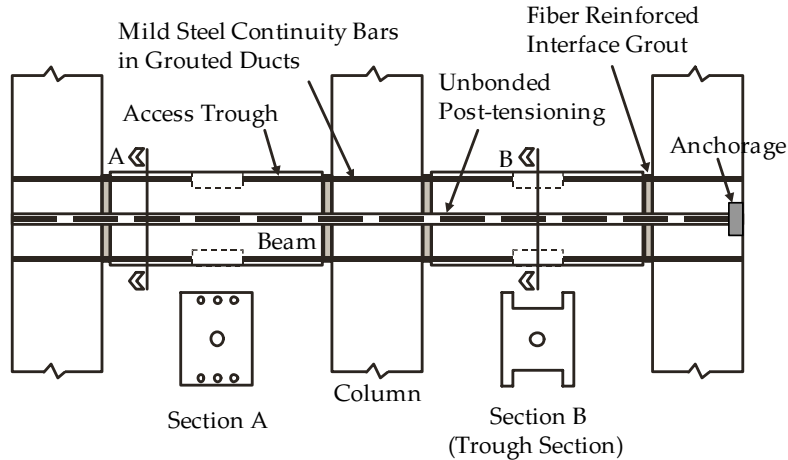


Figure 1. Hybrid Frame Concept

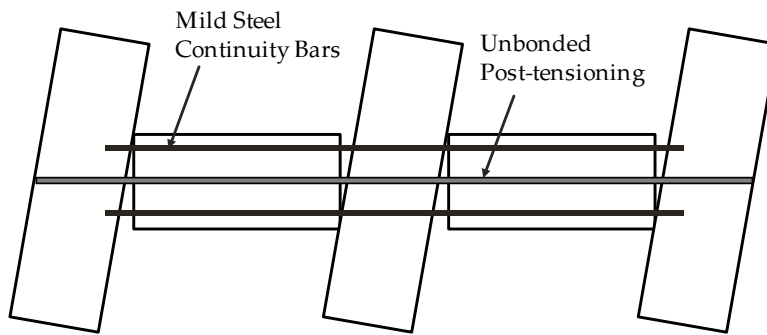


Figure 2. Hybrid Frame Under Lateral Load

interfaces. However, the tendon, being unbonded, remains elastic because the elongation is distributed over its entire length. Therefore, when the load is removed, the tendon restores the framing elements to their original, unloaded, configuration. Such a system would theoretically possess no damping. Thus, to prevent excessive displacements during the ground motion, energy dissipation is added by grouting deformed reinforcing bars in ducts at the top and bottom of the beams. Now, when the crack at the interface opens and closes, the bars are forced to yield alternately in tension and compression, providing the desired damping.

The flexural resistance is provided by two separate types of reinforcement, each of which has a distinct role to play. The unbonded tendons provide some of the resistance, and ensure that the frame is upright, without residual drift, at the end of the ground motion. The yielding reinforcement provides both addition flexural resistance and energy dissipation. This separation of the two functions (re-centering the frame and reducing the peak displacements by dissipating energy) is the key to its success. The same principle is used in an automobile suspension, in which the springs and shock absorbers are separate units, each with their own function to fulfill. In a conventional frame, reinforced with deformed bars alone, the bars either remain elastic, in which case the frame re-centers but no energy is dissipated, or they yield, in which case the

frame will, in general, not re-center. The bars cannot simultaneously yield and remain elastic, so they cannot fulfill both functions.

The primary advantage of the Hybrid Frame is that the structure can be made to re-center after an earthquake, and therefore to display essentially zero residual drift. In addition, precast concrete frames designed using this philosophy have shown significantly less damage than commonly occurs in conventional frames that are deformed to the same drift level (Priestley et al. 1999). Precast Hybrid frames also offer the usual benefits of precasting: high-quality finishes, good control of the concrete, speed of erection, and economy from repetitious use of formwork.

TEST PROGRAM

Test Specimens

The test program was carried out as proof-of-concept for the Hybrid Frame system, which had been selected for use in the Paramount Apartments in San Francisco (Englekirk 2002). The tests were carried out at the University of Washington because of that institution's role in developing the system, and therefore its familiarity with the frame's behavior. The tests were carried out in accordance with ACI-ITG1.1, even though at the time it existed only in draft form. All the test specimens were designed by the Engineer of Record for the prototype structure.

ACI-ITG1.1 requires testing of every basic configuration, such as interior, exterior or corner joint, that will be used in the prototype structure. Because the designer proposed to use some frames that were continuous round the corners of the building, a minimum of three specimens (one interior, one exterior and one corner) was necessary. In the end, two corner specimens were tested, to study different interior details. In one, separate tendons ran in each direction and crossed and were both anchored at the column, while in the other a single, continuous tendon was contained in a duct that had a 90° bend within the column. The specimens were approximately 2/3 full scale, and are shown schematically in Figure 3.

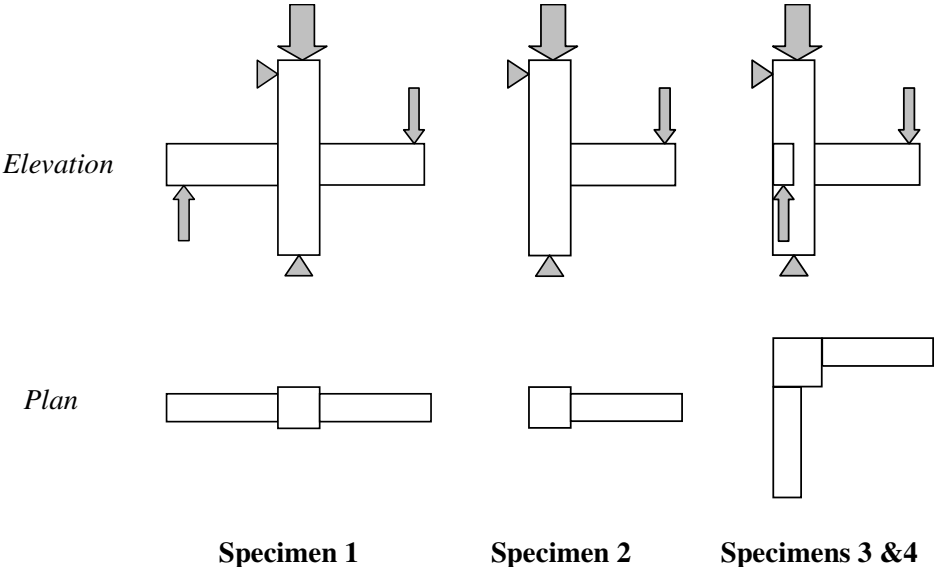


Figure 3. Test Specimens

Each consists of a beam-column sub-assembly, made from a single column element and either one or two beams. In the interests of simplicity, slabs were not included in the tests.

The proportions of the frame followed those used in the prototype, and the columns were made slightly wider than the beams, for both architectural and other reasons. Dimensions are shown in Table 1. The heights of the columns and the lengths of the beams were chosen so they could be supported at locations that represented the points of inflection in the prototype, thereby achieving the correct ratio of moment to shear in the members. One of the questions that arise in constructing a Hybrid Frame is how to insert the bars into the ducts at the top and bottom of the beams. In the tests, it was solved using a method proposed by Seagren (1993). The beams are made with a trough in the top and bottom surface (Figure 1) that extends over approximately the central half of the beam's length. The trough lines up with ducts at the beam ends, which in turn are aligned with the column ducts. The bars are located in the ducts and trough before lifting the beam into position, and they can then be moved by hand through the duct into their final position, thanks to the access provided by the trough. The trough is then filled with grout or concrete. This detail was used in the test structures, except that the troughs were not filled after inserting the bars.

Table 1. Specimen Dimensions (inches)

Specimen	1	2	3, 4
Beam height	21	21	21
Beam width	16	16	21
Beam length ¹	72	72	72
Column depth	20	20	24
Column width	18	18	24
Column height ²	120	120	120

Notes: 1. From center of column to loading point
2. Height between points of inflection

Test Setup

Figure 4 shows the test set-up for the corner specimens. The others were similar, but were simpler because the specimens were planar and required reaction bracing in one direction only. All specimens were tested against the University's L-shaped reaction wall. In the setup, the column remained vertical and each beam was loaded vertically by a servo-controlled hydraulic actuator located at the point of inflection near the beam tip. P-Δ effects were thus excluded from the test behavior. This is desirable, because they can best be added in software during subsequent frame analyses. Doing so allows the analyst to account for the variations in axial load that occur during the frame's response to the particular ground motion being used.

The column was seated on a multi-directional rotation bearing, and was secured at the top in each direction by a steel strut that contained an in-line load cell. The bearing provided a pin connection at the bottom, and the struts at the top contained rockers that ensured zero moment there as well. The column axial load was applied through a steel cross-beam on top of the column was stressed to the strong floor using high strength rods. The 110 kip actuators were

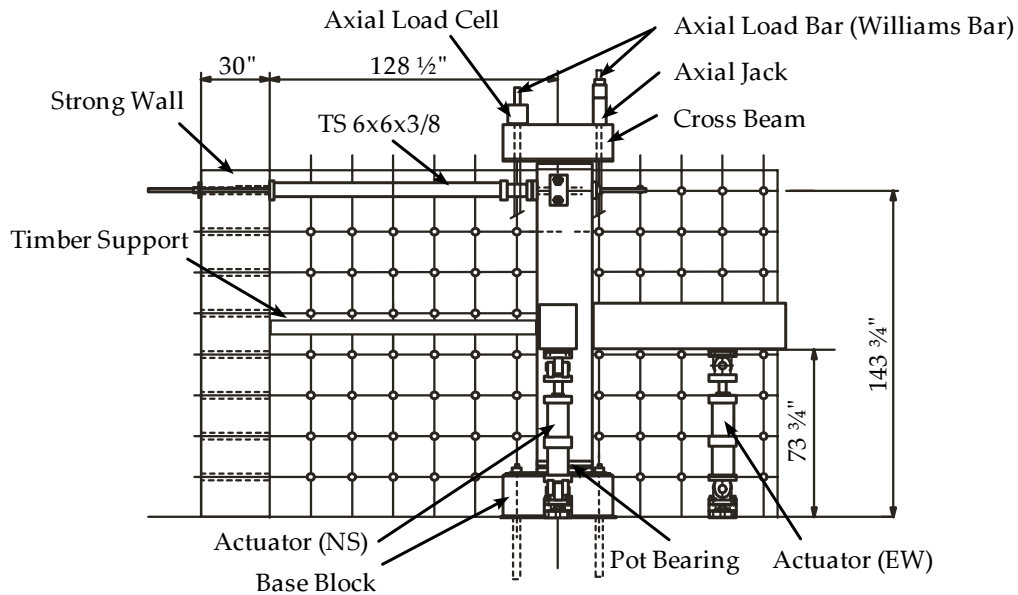


Figure 4. Test Setup for Specimens 3 and 4

connected to the beams using swivels. Height limitations precluded the use of load cells, so the actuator forces were obtained using differential oil pressure circuitry that was calibrated prior to the testing. Additional bracing was installed between the beams and strong wall to prevent any potential twisting of the column about the vertical axis. It was connected in such a way as not to inhibit vertical movement of the beams.

The individual concrete elements were fabricated by Charles Pankow Builders Ltd at their Midstate casting yard in California, and were assembled in the laboratory. The column was erected and braced first, then the beams were erected on temporary falsework, grouted with a fiber-reinforced grout, and then prestressed using a multi-strand post-tensioning ram. The bars were then inserted in the ducts and were grouted using high-strength grout without fibers.

The specimens were extensively instrumented. Internal strain gages were used on the longitudinal bars and ties in both the beams and column. These were installed at the precasting yard. Others were installed on the continuity reinforcement before it was installed in the ducts. Load cells were installed in the top braces, the cross-beam that applied the axial load to the column, and at the post-tensioning anchorages. Potentiometers and LVDTs measured displacements.

Loading Program

The loading regime consisted of cycles of applied displacements at the beam tips. The applied drift history for the corner specimens is shown in Figure 5. For the interior and exterior specimens, the history followed the requirements of ITG1.1 exactly, and consisted of sets of three identical cycles, with the amplitude increasing of each set by approximately 25%. In the corner specimens, the procedure was slightly different. First, the applied displacements were the vector sum of the two directions. Second, two different displaced shapes are possible in the

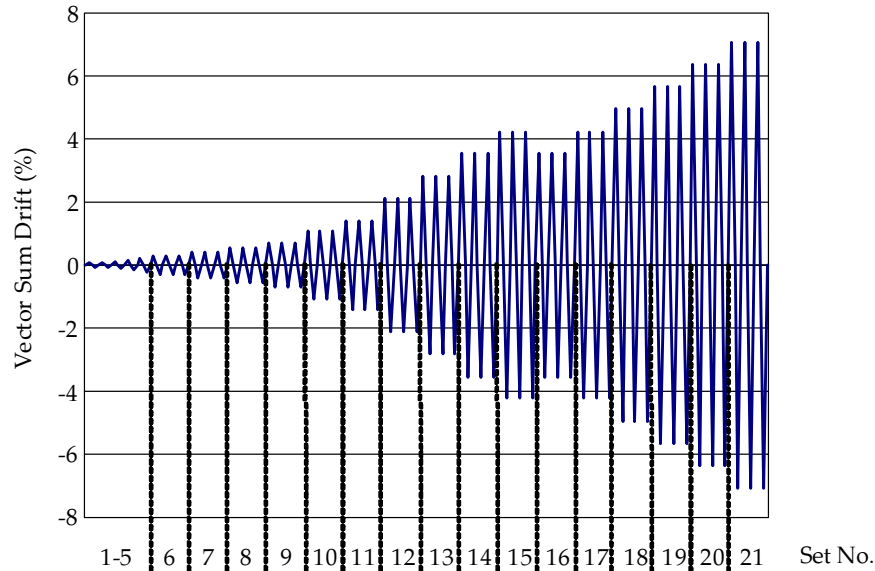


Figure 5. Applied Drift History (Specimen 4)

specimen. In the anti-symmetric one, one beam is pushed upwards while the other is pulled down, and in the symmetric one, both beams move in the same direction simultaneously.

The symmetric loading is harder to achieve in the laboratory because the column axial force changes significantly during the cycles unless it is actively controlled. Furthermore, the column force is different above and below the joint, so, if a nominal value of, say, $0.1f_c A_g$ is required, a decision must be made about where that force is to act. A further difficulty arises because the joint shear stress for a given drift ratio differs between the symmetric and anti-symmetric modes, being slightly higher for the former. (It also acts on a skew plane in a corner specimen). The procedure adopted here was to conduct most of the cycles using the anti-symmetric mode to simplify the testing, but to insert two extra sets of cycles (at 3.54% and 4.24% vector sum drift) in the symmetric mode, to demonstrate that the system had adequate joint shear capacity.

TEST RESULTS

ITG Requirements

ITG 1.1 imposes three acceptance criteria, all of which must be satisfied on the third cycle to 3.5% drift ratio:

- The strength of the specimen must be not less than 75% of the peak strength.
- The relative energy dissipation ratio (REDR) must be not less than 1/8.
- The secant stiffness between +0.3% and -0.3% drift ratio must be not less than 5% of the initial stiffness.

All four specimens satisfied these three requirements. It is worth noting that these requirements are, in fact very stringent, and that a conventional SMRF, designed in accordance with Chapter

21 of ACI 318, is not capable of satisfying them. This has been demonstrated by tests at NIST (Cheok and Lew 1990). Those tests were conducted prior to the publication of ACI-ITG 1.1 but followed a similar loading protocol. The two specimens were damaged beyond repair prior to reaching 3.5% drift ratio.

The REDR is related to the damping, and is defined by the area of the hysteresis loop divided by the sum of the areas of the two circumscribing parallelograms in the positive and negative force regions of the load-displacement plot, as shown in Figure 6a. The sides of the parallelograms are drawn parallel to the initial stiffnesses, which may be different in the positive and negative directions. By contrast, the equivalent viscous damping (EVD) is given by the area of the hysteresis loop divided by the area of the circumscribing rectangle (Figure 6b). The relationship between the REDR and the effects of energy dissipation on response is not as intuitive as is the case with the EVD. This is demonstrated by considering the response of an elastic-perfectly plastic system. At low drift ratios, when the system is still elastic, no energy is dissipated so the EVD is zero, but the REDR is indeterminate (i.e. 0/0). After yielding, the REDR is 100% for all values of ductility, μ , whereas the EVD is given by $(1-1/\mu)$, and therefore varies from 0% to 100% as the ductility varies from 1.0 to ∞ .

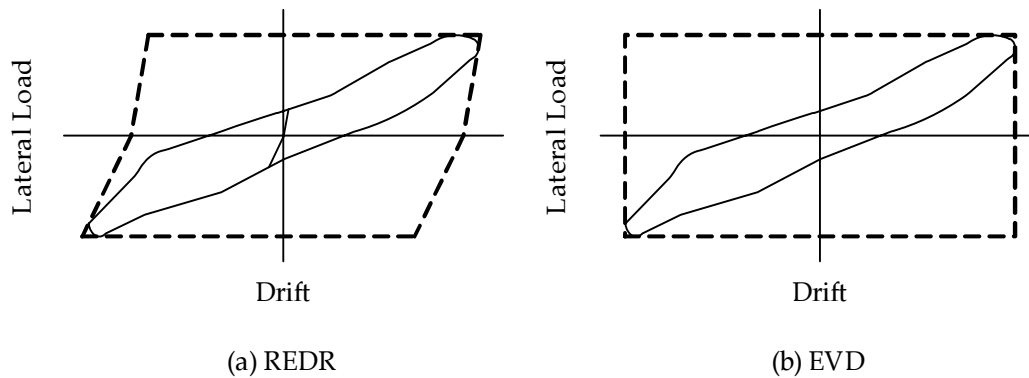


**Figure 6. Definitions of Damping: a) Relative Energy Dissipation Ratio (REDR)
b) Equivalent Viscous Damping (EVD)**

Observed Behavior – Global Behavior

The critical events shown in Table 2 were taken as measures of the behavior and were recorded for all specimens.

Table 2. Summary of Critical Events

Specimen	1	2	3	4
Joint cracking	0.3	0.15	0.14	0.6
Beam cracking	0.4	0.2	0.27	0.6
Grout cracking	0.4	0.1	0.4	0.2
Continuity bar yielding	1.0 - 1.5	0.75	1.0 - 1.3	1.1
Continuity bar fracture	NA	4	4.7	4.2
Joint spalling	3	NA	NA	NA
Beam spalling	NA	3.5	4	2.1
PT yielding	NA	NA	NA	NA

The peak loads and drift ratios are given in Table 3. The loads are expressed in terms of beam moments in order to provide a uniform basis for comparison among the four specimens, which had different numbers and configurations of beams. The beams were all nominally identical, and the coefficient of variation of the strengths is only 4%, despite the differences in configuration.

Table 3. Peak Responses

Specimen	1	2	3	4
Peak moment, average (kip-ft)	334	320	349	318
Peak drift (%)	6	4.5	4.5	6.5
Drift at 75% peak load (%)	3.5	4	4	4.5
Failure mode	joint shear	bar fract.	bar fract.	bar fract.

Failure was defined, arbitrarily, as a 25% drop in strength from the peak value. According to this definition, Specimens 2-4 failed by bar fracture, which typically occurred at approximately 4% drift. However, the specimen retained significant strength after the bar had fractured, because the PT was still elastic and resisting load. By contrast, Specimen 1 suffered extensive joint shear damage and no bars fractured. These failure mechanisms are discussed in greater detail below. The damage to the concrete consisted mainly of joint cracking, beam cracking, and some spalling. In all specimens except Specimen 1, it could have been repaired relatively easily by patching and epoxy injection.

Component Behavior

Interface

The system is intended to respond to lateral loads by lift-off of the beam from the grout bed at the beam-column interface. In all cases this occurred and, in Specimens 2-4, lift-off provided much the largest contribution to the total drift. Even in Specimen 1, it constituted half of the total up to a drift ratio of 3%, after which the joint shear deformations dominated. The interface grout was reinforced with polypropylene fibers, which held the grout in place when the beam lifted clear from the grout pad, even though it had previously been subjected to high stress. The

use of fiber reinforcement in the grout is critical to its performance. In general the grout at the top and bottom of the pad suffered some permanent compression due to the high local stress that existed there at peak rotation and, at the end of each test, its surface was slightly curved, rather than planar.

Beams

The beams experienced axial force (from the PT), moment and shear. They generally cracked in two places: near the beam-column interface where the moment was highest and at the ends of the troughs where the sharp corner of the breakout caused a stress concentration. The cracks near the interface were dominated by flexure, whereas those starting at the breakout were oriented at an angle, indicating the effects of shear. Because of the reduced concrete area near the trough, and the difficulty of using complete closed hoops there, that region must be detailed carefully if the shear cracks are not to become excessively wide. The widths of the beam cracks in the tests never exceeded approximately 0.04 inches (1 mm), and they had no detectable influence on the structural response.

In Specimen 2, the cover spalled at the bottom of the beam at 4% drift, as shown in Figure 7, which also shows the gap opening. Similar spalling occurred in one beam of Specimen 3. As can be seen, there was almost no other damage, and, in both cases, the damage could have been repaired easily, and the frame could have been classified as ready for Immediate Occupancy, despite the large drift to which it had been displaced.

The transverse reinforcement in the beams remained elastic at all times. The highest recorded strain was approximately $1000 \mu\epsilon$, or half the yield strain. This behavior is due to the post-tensioning, which results in much of the beam shear to be carried by a single diagonal strut spanning from corner to corner of the beam (Stanton et al. 1997). In the absence of bonded

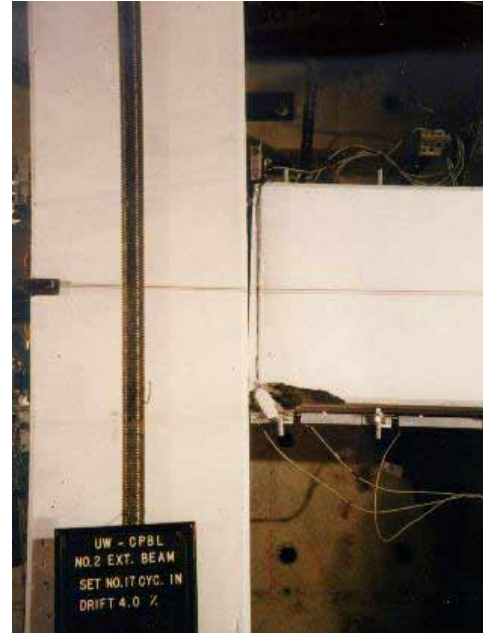


Figure 7. Cover Spalling of Specimen 2 at 4% Drift

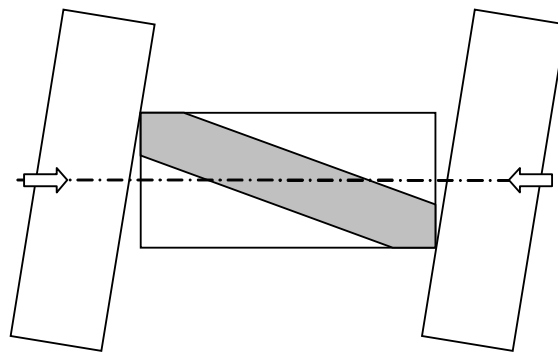


Figure 8. Shear in Hybrid Frame Carried by a Single Strut

continuity bars, this strut must carry all the shear, as shown in Figure 8. Transverse reinforcement is thus needed only for the confinement of the strut, and it is needed primarily at the beam end. This behavior stands in contrast to that of a conventional frame containing bonded reinforcement, in which shear forces are all carried by a truss mechanism, which leads to yielding of the stirrups and extensive shear damage.

Joint Cracking

In all cases, the joint cracked due to the joint shear stress demand. The drift at which this occurred is given in Table 2. Specimen 1 (interior) suffered considerable joint shear damage. Two major diagonal cracks were apparent at 2.5% drift, and thereafter the concrete in the joint degraded. However, it did so in a manner that was very different from that seen in a conventional frame joint. The 3" diameter post-tensioning duct ran horizontally through the joint at mid-height and, because of the void that it created, it reduced the plan area available for resisting the joint shear force. The joint damage was concentrated within a 3" high horizontal band across the joint that coincided with the duct.

The damage is attributed to the fact that computed joint shear stress was $21\sqrt{f'_c}$, compared with the $\phi 15\sqrt{f'_c}$, or $13.75\sqrt{f'_c}$, permitted by ACI 318. (This value is based on ACI 318-99. In 2002, the ϕ factor was reduced, but the overstrength factor of 1.25 on the bar yield force remained unchanged, so the permissible joint shear stress was reduced effectively to $11.25\sqrt{f'_c}$. The joint shear stress in the specimen was thus almost twice the contemporary allowable value). The computed value was based on the ultimate strength of the deformed bars, measured in separate coupon tests, the force in the post-tensioning tendon measured from the load cell, and the net area of concrete.

In Specimens 2 (exterior) and 3 (corner), local stresses due to the post-tensioning anchor head caused some hairline cracking in the joint before the lateral loading was applied. The cracking recorded in Table 2 does not include this, and is restricted to external load-induced cracking.

In none of the other specimens did joint shear cause significant deformation or damage, largely because the joint shear stress was lower. Specimen 2 had only one beam, and therefore the joint shear force demand was smaller, but it is believed that the beneficial presence of the PT anchor head also caused the diagonal strut to be flatter, and therefore the force in it to be lower, than would be the case for an interior joint. The corner columns were larger (24" × 24"), which reduced the joint shear stress in them. However, the beams were offset, which makes calculation of the true joint shear stress more complicated. The measured strains in the joint ties showed that some stress was carried even by the concrete at the inside face of the joint, furthest from the beam centerline. The rules in ACI 318-02 for determining the joint area exclude this region, and so appear somewhat conservative. The degree of conservatism could not readily be determined from the evidence available from only two specimens with relatively unusual internal details.

Continuity Bars

The continuity bars were all debonded for a length of 9" ($12d_b$) in the beam, next to the interface, in order to prevent premature fracture. Subsequent experiments (Raynor et al. 2002)

have shown that bars grouted in ducts experience much higher bond stresses than do bars embedded directly in concrete because of the confinement provided by the duct. In reinforced concrete beams, the cracks are distributed and the bar experiences additional debonding due to yielding, that is sometimes referred to as “strain penetration”. This behavior distributes the bar strains and reduces the peak value. In a precast system, the crack is concentrated at the interface and the additional debonding due to yielding is small, so a short length of the bar must be deliberately debonded if premature fracture is to be avoided. If the lever arm between the neutral axis and the bar is taken as approximately $(2/3)h$, then the strain can be computed as

$$\varepsilon = \left(\frac{2h}{3} \right) \frac{\theta}{L_u} \quad (1)$$

where h is the beam depth, θ is the interface rotation angle (approximately equal to the drift), and L_u is the unbonded length of the bar. For $h = 21''$ and $L_u = 9''$, as used here, Equation 1 implies that bar fracture occurred at approximately 4% strain. This is much lower than the specified elongation at break for ASTM A706 bars, and the difference is attributed to the effects of cyclic loading. Equation 1 also shows that the drift at which the bars start to fracture can be increased by increasing L_u .

Post-tensioning

In no case did the post-tensioning yield. The largest loss of post-tensioning at the end of the test, measured using the load cells, was 7%, and is attributed to slip-back loss as the anchors seated completely and to compression of the grout pad. Because the tendons in the tests were much shorter than would be the case in the field, the seating loss was much more severe. The post-tensioning was at all times sufficient to prevent vertical slip of the beams against the grout pad.

DISCUSSION

In all specimens, the beams lifted off from the columns to provide a significant proportion of the total drift, the continuity bars yielded and the post-tensioning remained elastic. These three features are consistent with the intended behavior. Furthermore, the damage to the beams and columns was slight and was easily repairable.

The behavior of Specimen 1 differed from that of the other three and provided some insights into joint shear behavior. First, joint failure in conventional frames is characterized by the formation of large diagonal cracks through the joints and break-up of the entire joint region. Here, however, the cover was lost over the entire joint region, but thereafter the damage was restricted to a zone that lay either side of the PT duct. The reduction in joint area caused by the duct clearly had a significant influence in raising the stress. Second, yielding of the continuity bars in conventional frames causes a partial but progressive loss of bond (Walker et al. 2004), which reduces the lever arm of the beam moment and therefore increases the joint shear stress, thereby hastening the demise of the joint. In a precast frame, the bond of the continuity bars is improved by the presence of the ducts. Inspection of the test specimens after the tests showed that debonding of the bars had penetrated only about an inch into the column, so it had had almost no effect on the joint shear behavior. This finding suggests that the behavior of joints in

conventional frames could be improved by improving the bond of the continuity bars, perhaps by providing confinement.

The grout deformed plastically at the top and bottom of the pad at the interface. This deformation served to protect the beams by reducing the high local stress that would otherwise have existed at the extreme face. The use of fiber reinforcement is essential to the plastic behavior. Furthermore, it is argued here the damage to the beams can be minimized by using a grout with a strength lower than that of the beam concrete. The true stress that can be carried on the grout is higher than the cube strength of the material because the pad is relatively thin compared with its other dimensions and so is confined very effectively by the adjoining beam and column faces. Separate tests (Chiu 1998) have shown that the confinement raises the grout strength by a factor of at least 2, even if it contains no fibers.

It is therefore believed that section 6.3.2 of ACI-ITG 1.2, which requires that the grout strength be at least equal to the concrete strength, is misguided. It is likely to provide no structural benefit, but is likely to impose the drawback of unnecessary damage to the beam ends. A better approach is to provide good confinement to the beam ends, and grout that is fiber-reinforced but has a nominal strength that is slightly lower than that of the concrete. This approach uses the principles of Capacity Design to protect the beam ends. The confining steel in the beam ends should also contain as much of the concrete as possible because the cover, which is by definition unconfined, is prone to damage. Custom-made welded bar grids are ideal for the purpose. They are preferable to spirals because they simplify fabrication of the beam cage and they enclose more of the concrete.

In Specimens 2 (exterior) and 3 (corner), local high stresses at the post-tensioning anchorages caused some hairline cracking in the joint before the lateral loading was applied. These cracks did not propagate significantly during the loading. The joint dimensions should be selected to ensure that space exists for both the anchorage head itself and adequate confinement steel to control the cracking associated with these local stresses.

ACI-ITG 1.1 requires that the test specimens provide an REDR of at least 12.5% at a drift ratio of 3.5%. All four specimens satisfied this requirement. However, it is argued here that the requirement is both unnecessary and could inhibit the development of new framing systems. While there is a clear need for damping in a seismic frame, it is a system property and not one that needs to be satisfied on a joint-by-joint basis. For example, the damping could be supplied by viscous or friction dampers that are located some distance from the beam-column joints and the frame could display excellent response.

CONCLUSIONS

Tests were conducted on four Hybrid Frame beam-column specimens. All four specimens satisfied the requirements of ACI-ITG 1.1, which address strength stiffness and energy dissipation.

In three of the specimens, the damage was minimal, even after they had been deformed to drift ratios between 4.5% and 6%. In the fourth specimen, the joint shear stress was almost twice the value allowed by ACI 318-02, and consequently the joint suffered considerable damage.

In all four specimens the post-tensioning remained elastic, and the deformed bars yielded, throughout the test. The measured behavior was thus in accordance with the intended behavior.

REFERENCES

- “2003 International Building Code”. (2003). International Code Council, Falls Church, VA.
- “Building Code Requirements for Structural Concrete (ACI 318-02) and Commentary (ACI 318R-02)”. (2002). Committee 318, ACI, Farmington Hills, MI.
- “Uniform Building Code, Vol. 2”. (1997). International Conference of Building Officials, Whittier, CA. 492 pp.
- ACI Innovation Task Group 1 and Collaborators (ACI ITG/T1.1-01). (2001). “Acceptance Criteria for Moment Frames Based on Structural Testing”. American Concrete Institute, Farmington Hills, Mich. 10 pp.
- ACI Innovation Task Group 1 and Collaborators (ACI ITG/T1.2-03). (2003). “Special Hybrid Moment Frames Composed of Discretely Jointed Precast and Post-Tensioned Concrete Member (T1.2-03) and Commentary (T1.2R-03)”. American Concrete Institute, Farmington Hills, Mich. 15 pp.
- Cheok, G. S. and Lew, H. S. (1990). “Performance of 1/3 Scale Model Precast Concrete Beam-Column Connections Subjected to Cyclic Inelastic Loads”. Report No. NISTIR 4433, Building and Fire Research Laboratory, NIST, Gaithersburg, MD. 94 p.
- Cheok, G. S. and Stone, W. C. (1994). “Performance of 1/3 Scale Model Precast Concrete Beam-Column Connections Subjected to Cyclic Inelastic Loads – Report No. 4”. Report No. NISTIR 5436, Building and Fire Research Laboratory, NIST, Gaithersburg, MD. 59 p.
- Chiu, P. (1998). “Fundamental Behaviors of Grout under Compressive Load and Moment”. Independent Study Report, University of Washington, Seattle, WA. 33p.
- Christopoulos, C., Filiatrault, A., Uang, C.-M., and Folz, B. (2002). “Posttensioned Energy Dissipating Connections for Moment-Resisting Steel Frames”. *Jo. Struct Engrg.*, 128(9), pp. 1095-1240.
- Englekirk, R. E. (2002). “Design-Construction of the Paramount – A 39-Story Precast Prestressed Concrete Apartment Building”. *PCI Jo.* 47(4), pp 56-71.
- Ishizuka, T., Hawkins, N. M., and Stanton, J. F. (1984). “Experimental Study of the Seismic Resistance of a concrete Exterior Column Beam Sub-assembly Containing Unbonded Post-Tensioning Tendons”. Dept. of Civil Engineering, University of Washington, May.
- Nakaki, S. D., Stanton, J. F., and Sritharan, S. (1999). “An Overview of the PRESSS Five Story Precast Test Building”. *PCI Jo.*, 44(2), pp. 26-39.

- Priestley, M. J. N. and MacRae, G. A. (1996). "Seismic Tests of Precast Beam-to-Column Joint Subassemblages with Unbonded Tendons". *PCI Jo.*, 41(1), pp. 64-81.
- Priestley, M. J. N., Sritharan, S., Conley, J. R., and Pampanin, S. (1999). "Preliminary Results and Conclusions from the PRESSS Five-Story Precast Concrete Test Building". *PCI Jo.*, 44(6), pp. 42-67.
- Raynor, D. J., Lehman, D. L., and Stanton, J. F. (2002). "Bond-Slip Response of Reinforcing Bars Grouted in Ducts". *ACI Struct. Jo.*, 99(5), pp. 568-576.
- Ricles, J. M., Sause, R., Garlock, M. M., and Zhao, C. (2001). "Post-tensioned Seismic-Resistant Connections for Steel Frames". *Jo. Struct. Engrg.*, 127(2), pp. 113-121.
- Seagren, D. (1993). Personal Communication with John Stanton.
- Stanton, J. F., Stone, W. C., and Cheok, G. S. (1997). "A Hybrid Reinforced Precast Frame for Seismic Regions". *PCI Jo.*, 42(2), pp. 20-32.
- Stanton, J. F. and Nakaki, S. D. (2002). "Design Guidelines for Precast Concrete Seismic Structural Systems". PRESSS Report No. 01/03-09. Also Published as University of Washington Report No. SM 02-02.
- Stone, W. C., Cheok, G. S., and Stanton, J. F. (1995). "Beam-Column Connections Subjected to Cyclic Loads". *ACI Struct. Jo.*, 92(2), pp. 229-249.
- Walker, S. G., Yeargin, C. M., Lehman, D. E., and Stanton, J. F. (2004). "Seismic Performance of Reinforced Concrete Beam-Column Joints without Joint Reinforcement". Accepted for publication by ACI Structural Journal.